

Spin canting, surface magnetization, and finite-size effects in γ -Fe₂O₃ particles

F. T. Parker, M. W. Foster, D. T. Margulies, and A. E. Berkowitz

Center for Magnetic Recording Research, 0401, University of California, San Diego, La Jolla, California 92093-0401

(Received 16 December 1991)

Small γ -Fe₂O₃ acicular particles (250-Å diam by 2000 Å) with and without surface coating of ⁵⁷Fe were examined by Mössbauer spectroscopy in large (to 60 kOe) longitudinal applied fields. As has been previously seen, the Fe moments are not aligned in large fields. However, unlike previous results, the canting is found to be a finite-size effect rather than a surface property. Magnetization versus field curves for the uncoated small γ -Fe₂O₃ particles and, as a comparison, large γ -Fe₂O₃ particles were analyzed with log-normal anisotropy field distributions within the Stoner-Wohlfarth model. The small particles show a large paramagnetic susceptibility that increases with decreasing temperature. Using a Langevin-function analysis, one finds that the susceptibility is not due to superparamagnetism, and the susceptibility correlates well with the Mössbauer canting. Hyperfine-field tailing increases with temperature for the small particles, especially for the coated samples, indicating weaker surface exchange interactions.

INTRODUCTION

It has been generally accepted¹ that the surface spins of fine particles of some ferrimagnetic oxides are canted to a much greater degree than those of the core, i.e., the net moment does not align with large fields. Coey² reached this conclusion from his studies of extremely small γ -Fe₂O₃ particles. Using Mössbauer spectroscopy, he showed that small γ -Fe₂O₃ particles do not saturate at 4.2 K even in a 50-kOe field. To determine whether the canting occurred primarily on the surface or in the core of the particles, Morrish *et al.*³ examined a γ -Fe₂O₃ powder sample that had been coated with isotopically enriched ⁵⁷Fe, the Mössbauer isotope. Since natural Fe contains only 2.2% ⁵⁷Fe, the resultant Mössbauer spectra were surface weighted. In longitudinal (along the γ -ray propagation direction) applied fields, the second and fifth lines were enhanced relative to the other four lines compared to the untreated powder, indicating larger canting for the coated powder. Although there was some experimental difficulty with the treatment, resulting in some very small particles yielding unsplit superparamagnetic lines, the authors concluded that the canting occurs primarily on the surface. In agreement with this model, small particles with high ratios of surface area to volume show enhanced canting relative to larger particles when measured with the same values of applied field and temperature.⁴ Other investigators using similar techniques have also attributed the observed canting to a surface phenomenon in γ -Fe₂O₃ (Refs. 5 and 6) and the same conclusion was reached about NiFe₂O₄ and CoFe₂O₄ particles.^{7,8} However, we have recently demonstrated⁹ that there is no preferential surface canting on Co-adsorbed γ -Fe₂O₃ in small applied fields. This was shown to be consistent with a theoretical model which included the high surface magnetocrystalline anisotropy energy associated with Co.

Since the coated materials of Ref. 3 show states other than those associated with magnetically stable γ -Fe₂O₃,

we have reexamined the matter. In this work, we report data demonstrating that the observed canting in γ -Fe₂O₃ particles is not a surface effect, but a finite-size volume effect. The surface spins do, however, exhibit a weaker exchange than is found in the core states.

Mössbauer spectra of small γ -Fe₂O₃ particles with and without ⁵⁷Fe coating were obtained in longitudinal applied magnetic fields. The relative areas of the Mössbauer lines are in the ratio 3:2*p*:1:1:2*p*:3,¹⁰ where the polarization (*p*) is related to the canting angle (θ) between the moment and the γ -ray propagation direction for a single spin direction by $p = 2 \sin^2 \theta / (1 + \cos^2 \theta)$. The spectra were fit with distributions in magnetic hyperfine field allowing the determination of the Fe fraction with hyperfine fields (or moments) less than core values. The temperature and field dependence of these fractions provide data on weakened surface exchange and superparamagnetism. The canting observed in Mössbauer spectroscopy should be reflected in the magnetization vs field behavior of the particles. Experimental magnetization data are compared to a model based on coherently rotating particle moments. These calculations also yield data on possible superparamagnetic components, and on anisotropy field distributions needed for determination of theoretical Mössbauer polarization.

EXPERIMENTAL PROCEDURES

γ -Fe₂O₃ acicular particles (250 Å diam by 2000 Å) were coated with isotopically enriched iron (95% ⁵⁷Fe, obtained by acid dissolution of metal powder) in basic solution at 100°C for two hours. All wet procedures were done under Ar. Several preparations were made, resulting in similar room temperature Mössbauer spectra. Unless otherwise stated, the term "treated" refers to a sample with 2% metal ⁵⁷Fe coated. Mössbauer spectra were obtained on samples usually dispersed in benzophenone, using a superconducting magnet, with the field along the γ -ray propagation direction. The isomer shift reference is Fe metal at room temperature. Magnetiza-

tion measurements were obtained with a vibrating sample magnetometer on samples tightly wrapped in Ag foil.

MÖSSBAUER DATA FITTING PROCEDURES

The fit distributions in magnetic hyperfine field H are described with relative probability $P(H)$. All subspectra had a common polarization, and all lines had pseudo-Lorentzian shapes with common exponent.¹⁰ To account for preferential broadening of the outer subspectral lines due to unresolved hyperfine interactions and the discrete distribution spacing, a variable term proportional to the distance of a line from the center of its subspectrum was added to the common half width at half maximum (HWHM) parameter for all lines. The typical fit increase in the outer line HWHM relative to that of the inner line was about 10%. By renormalizing the height parameters, the relative areas under each line were left unchanged by this procedure. To partially eliminate the problem of line saturation in spectra obtained in applied fields, the two most intense subspectra were treated differently. These subspectra, denoted by "main," are primarily due to Fe^{3+} in the A and B sites of the particle cores. Their 1–6 line intensities were scaled by a separate free fit variable, typically about 0.95. These lines thus did not enter directly into the determination of p . For calculations with applied field (H_a) of 60 kOe, the hyperfine fields and isomer shifts (IS) of the two main subspectra were free variables. The other subspectra in the fits (denoted by "tail") were on two fixed distributions beginning 26 kOe above and below the H for each main subspectrum. The IS of the tail subspectra were set equal to those of the corresponding main subspectra. For the 60-kOe applied field, 296-K spectra, the IS of the tail subspectra for H below about 300 kOe were set equal to the weighted IS average for the main subspectra. For fits with data obtained at 40- and 20-kOe applied fields, the tail heights were fixed by the ratios relative to the main heights obtained with 60-kOe data, with the corresponding values of H adjusted for the change in external field.

For the spectra obtained with $H_a = 10$ kOe the two main spectra strongly overlap and unique fit parameters cannot be obtained by using the previous technique. Thus, two constraints were employed. The ratio of the two main subspectra intensities was fixed at about 1.5, as seen in the spectra obtained with $H_a = 60$ kOe at 4.2 and 296 K. The isomer shift separation of the two main subspectra was fixed at about 0.13 mm/sec, as found in the high-field measurements. The tailing subspectra were placed on a single fixed distribution 26 kOe above and below the highest H and lowest H main subspectra, respectively. The IS of these tailing subspectra were fixed at the weighted average obtained for the main subspectra.

Spectra obtained with $H_a = 0$ kOe were fit with a distribution similar to that used with data obtained in $H_a = 10$ kOe. Quadrupole splitting was allowed for the main subspectra and the three most intense tailing subspectra. Correlated main subspectra isomer shifts were used above in the fits of data obtained in 10-kOe applied field. With applied fields, the quadrupole shift essentially averages to

zero, although some fit line shift may occur.¹¹ Thus, in the fits for the $H_a = 0$ spectra, the main isomer shifts were both used as free parameters. Additionally, no attenuation factor was used on the main 1–6 lines.

RESULTS AND DISCUSSION

Representative Mössbauer data and fits are shown in Figs. 1 and 2, and $P(H)$ curves in Figs. 3 and 4. The

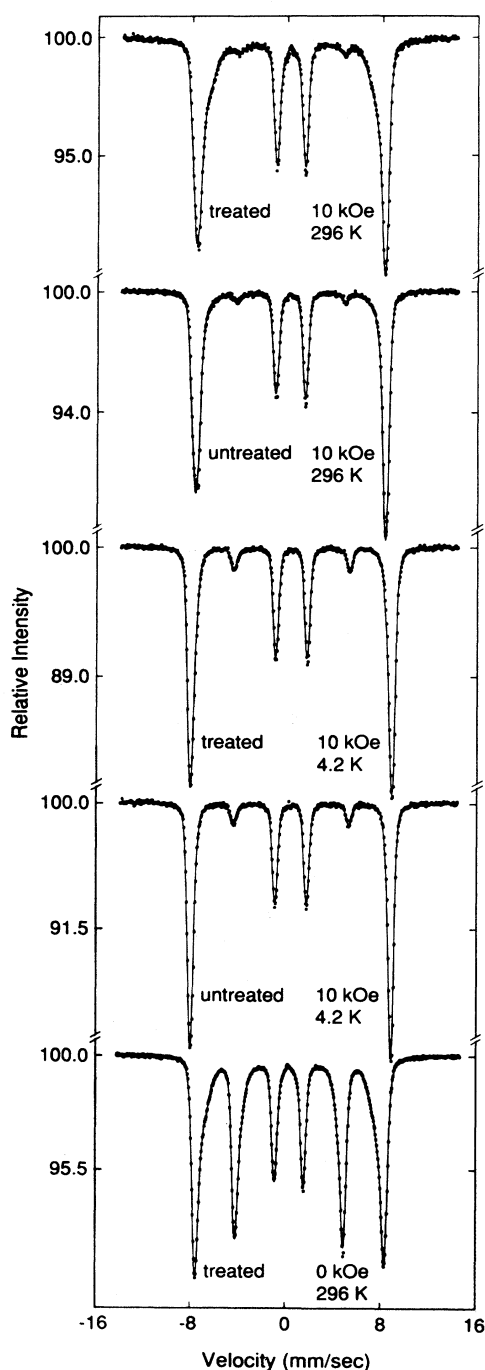


FIG. 1. Representative Mössbauer data obtained for treated (coated with 2% metal ^{57}Fe) and untreated $\gamma\text{-Fe}_2\text{O}_3$ in 10- and 0-kOe applied fields. The solid lines denote fits.

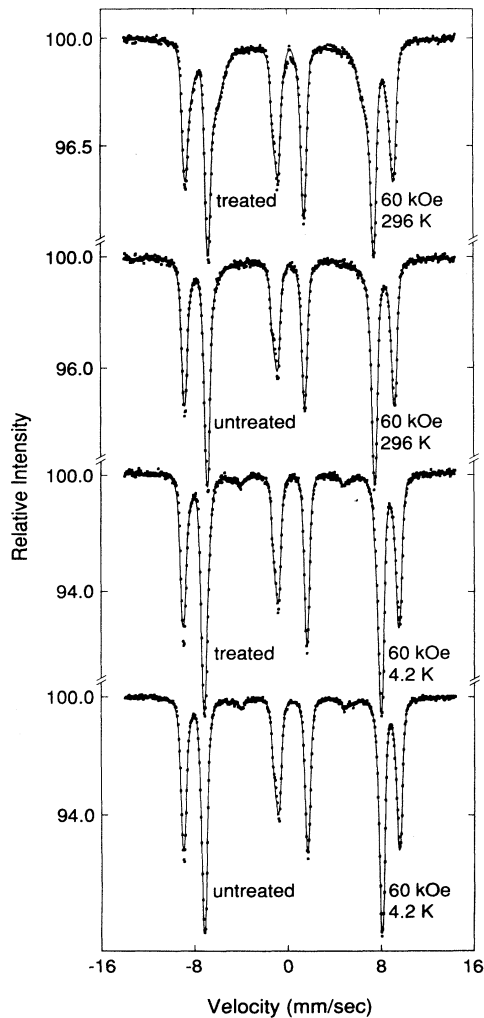


FIG. 2. Mössbauer data and fits obtained in 60-kOe applied field.

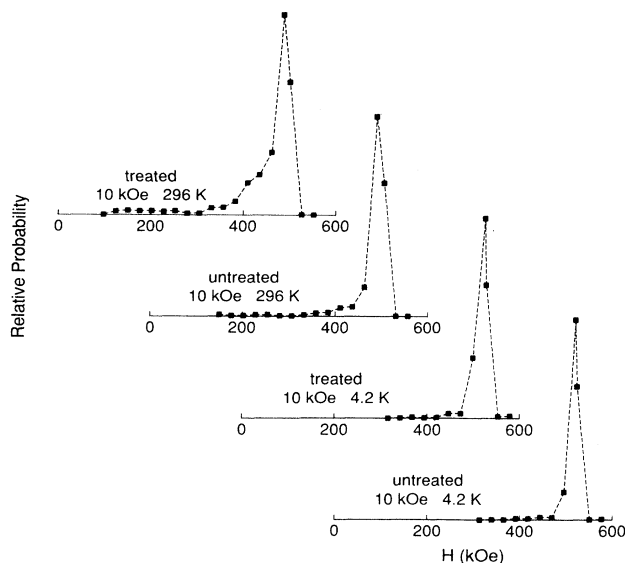


FIG. 3. Mössbauer hyperfine field distributions $P(H)$ for data obtained in a 10-kOe field. Dashed lines are visual guides.

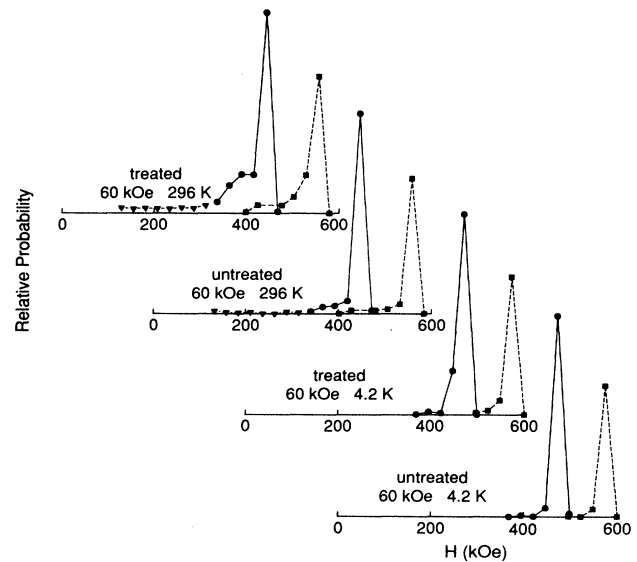


FIG. 4. $P(H)$ for data obtained in 60-kOe field. The lines are visual guides, connecting regions with common isomer shift. The isomer shift for the low-field values of $P(H)$ is the weighted average of the two high-field values.

Mössbauer area per mg of sample for the treated sample is double that of the original, as expected if all the ^{57}Fe coats the surface of the particles. There are many obvious similarities between the treated and untreated samples, especially at low temperature. The relative areas of the main A - and B -site peaks, their hyperfine parameters, and values of polarization are very similar, with no evidence of Fe^{2+} in the treated sample. These facts indicate that the added ^{57}Fe is on the particles, and in the form of $\gamma\text{-Fe}_2\text{O}_3$. There is no indication of $\alpha\text{-Fe}_2\text{O}_3$ on the surface of the particles, since $\alpha\text{-Fe}_2\text{O}_3$ does not show splitting into A and B subspectra in large applied fields.¹² By contrast, $\alpha\text{-Fe}_2\text{O}_3$ has been observed on the surface of thin films of $\gamma\text{-Fe}_2\text{O}_3$.¹³ In this latter case, the high temperature (300 °C) used to convert the films from Fe_3O_4 to metastable $\gamma\text{-Fe}_2\text{O}_3$ probably¹⁴ began the γ -to- α transition, which initiates on the surface.¹⁵

The fit values for polarization are the same for the treated and untreated samples at all temperatures (Fig. 5) and all fields (Table I). In 60 kOe, both samples show $p=0.06$ at 4.2 K, and essentially zero at 296 K. This thickness of the ^{57}Fe oxide shell is about 1.3 Å, if assumed uniform. If this surface layer were to conform to the previously hypothesized random state,⁴ and the core were aligned in field, the composite polarization would be 0.40, far greater than observed. Thus, we conclude that the observed canting is not a surface effect but is a size-dependent volume phenomenon.

The difference in these results from the previous Fe coating experiment lies in the presence of nonmagnetic central hyperfine peaks at room temperature in the previous work.³ These peaks indicate fast superparamagnetic relaxation, and thus the presence of some very small particles produced by the coating process, in addition to the larger particles, which were being coated. At low tem-

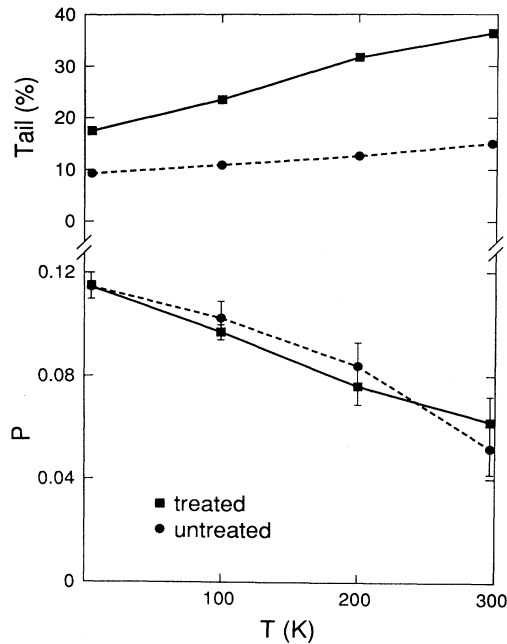


FIG. 5. Mössbauer polarization (p) and tailing fraction in a 10-kOe applied field vs temperature. Lines are visual guides.

perature, the smaller particles became magnetically stable and exhibited the split hyperfine pattern in zero applied field. Since they were smaller, they exhibited larger canting angles in applied field.⁴ The composite effective canting angle at a given applied field and temperature was thus larger than that for the uncoated particles. The present treated sample shows no evidence of nonmagnetic peaks at 296 K, even in zero applied field (Fig. 1), and even though the Mössbauer spectra are weighted towards the smaller particles due to the $1/d$ (d =diameter) dependence of the surface-to-volume ratio.

The largest difference in the Mössbauer data between the treated and untreated samples is the substantially greater tailing in the treated γ -Fe₂O₃ sample, as can be seen in Fig. 5. The tailing fraction is defined as the ratio of the Mössbauer area contained in the subspectra other than the two main subspectra to the total area. For both samples, the tailing increases with temperature, indicating a weaker exchange for the atoms comprising the tailing, possibly due to lower coordination in surface sites. The exchange interaction was estimated from the temperature response of the magnetic hyperfine field in a 10-kOe

applied field, assuming proportionality between atomic spin and hyperfine field. Boltzmann distribution mean-field sums were employed, with $g=2$, $S=\frac{5}{2}$. The core moments at the two main sites at 296 K averaged about 95% of their value at 4.2 K. This yields a mean core molecular field at room temperature of about 5000 kOe. For calculation of a typical surface value of molecular field, the diffuse peak in H at about 400 kOe for the treated sample at 296 K is ≈ 0.8 times the value at 4.2 K, and yields a room-temperature molecular field of 2400 kOe. The approximately 50% reduction in molecular field at the surface relative to the core of the γ -Fe₂O₃ particles is comparable to that found from a study¹⁶ of ⁵⁷Fe obtained from the ⁵⁷Co parent coated on the surface of γ -Fe₂O₃. For both current samples, neither tailing fraction approaches zero at 4.2 K, so part of the tailing probably arises from weaker core polarization or surface dipolar fields which are not strongly thermally activated. A and B sites show similar fractional tailing, although subspectral overlap reduces quantitative accuracy. The fractional tailing seems independent of applied field. For example, the treated sample shows 40, 36, and 41% tailing at 60, 10, and 0 kOe and 296 K. This rules against superparamagnetism as a tailing mechanism. For comparison and as a check on the fitting procedure, much larger γ -Fe₂O₃ particles (0.2 by 1 μ m) were found to exhibit less than 2% tailing (the statistical limit) in zero applied field at 296 K.

Another sample of the same small particle γ -Fe₂O₃ precursor was coated with 10% metal ⁵⁷Fe. More than 80% of the Mössbauer signal thus came from the surface of the particles. There were no evident paramagnetic peaks in zero applied field at 296 K. Spectra obtained in 60 and 10 kOe fields at 4.2 K showed statistically the same values of p as the other samples.

Temperature-dependent magnetostriction of materials based on γ -Fe₂O₃ is known¹⁷ to occur when these materials are embedded in organic binders. To test the possibility of this mechanism inducing the larger canting observed at low temperature, a sample of small-particle γ -Fe₂O₃ was ultrasonically dispersed in boron nitride powder. The observed values of p in 60 and 10 kOe fields at 4.2 K were the same as for the samples embedded in benzophenone.

MAGNETIZATION COMPARISON

For the untreated sample, moment vs field data in the first quadrant were fitted to a distribution in anisotropy

TABLE I. Comparison of some polarization values for γ -Fe₂O₃ and treated γ -Fe₂O₃ particles.

	H_a (kOe)			
	10	20	40	60
$T=4.2$ K				
γ -Fe ₂ O ₃	0.115(5)	0.081(3)	0.065(4)	0.056(4)
Treated γ -Fe ₂ O ₃	0.116(3)			0.058(4)
$T=296$ K				
γ -Fe ₂ O ₃	0.052(10)			0.028(12)
Treated γ -Fe ₂ O ₃	0.062(10)			0.011(8)

fields (H_K) using the Stoner-Wohlfarth model.¹⁸ This model assumes randomly oriented single-domain particles with coherently rotating moments. As a comparison, data for the large-particle γ -Fe₂O₃ (0.2 μ m diam by 1 μ m length) were similarly fit. The calculations were similar to those previously reported,¹⁹ except the saturation magnetization M_S was treated as a fit variable and a paramagnetic term was added. If the latter term was sufficiently large, then the Langevin formalism was used, with two paramagnetic variables. Thus, the calculated moment at given applied field (H_a) and temperature (T) is

$$m(H_a) = \frac{k_S \sum_{H_K} P(H_K) m(h)}{\sum_{H_K} P(H_K)} + m_p,$$

where m is the moment ratio to that observed at the maximum applied field (20 kOe), k_S the ratio of M_S to the moment observed at 20 kOe, $h = H_N/H_K$, and $H_N = H_a - \lambda m_e(H_a)$ with m_e the experimental moment ratio to that observed at 20 kOe applied field. The term λm_e is a small correction term to account for deviations of $m_e(0)/k_S$ from the expected Stoner-Wohlfarth value 0.5. The paramagnetic term is given by $m_p = \chi H_a$ for a linear differential susceptibility, or $m_p = k_{SL} L(a_L)$, with k_{SL} the saturation of the paramagnetic fraction, $L(a_L)$ the Langevin function, and $a_L = \mu H_a / kT$. $P(H_K)$ was assumed to follow a log-normal distribution with geometric mean anisotropy field $\langle H_K \rangle_G$ and geometric standard deviation σ . About 700 values of H_K were employed in the sum.

Moment-vs-field data and fits at 4.2 K are shown in Fig. 6. The temperature dependence of the fit parameters is shown in Fig. 7. At room temperature, the mean anisotropy fields and standard deviations are similar for the large and small particle γ -Fe₂O₃. At lower temperature, $\langle H_K \rangle_G$ for the large γ -Fe₂O₃ tends to saturate, as would be expected with the dominate shape anisotropy dependent only on moment. For small γ -Fe₂O₃, $\langle H_K \rangle_G$ is anomalously linearly dependent on temperature. The large γ -Fe₂O₃ exhibits a small, temperature independent paramagnetism, which is about 0.7% of the moment observed at 20 kOe. Small γ -Fe₂O₃ shows a large

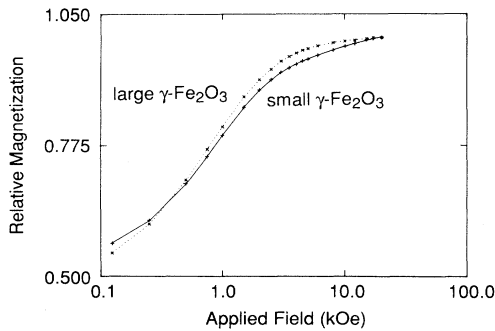


FIG. 6. Relative magnetization vs field at 4.2 K for small- and large-particle γ -Fe₂O₃. Lines denote the least-squares fits based on Stoner-Wohlfarth model.

temperature-dependent paramagnetic term, which increases with decreasing temperature to yield about 6% of the moment in 20 kOe at 4.2 K. However, a_L/H_a shows no temperature dependence. Thus, this magnetization component is not due to superparamagnetism.

The high-field paramagnetism is related to the Mössbauer canting. This can be seen by computing the equivalent change in angle for the average spin from the Mössbauer polarization, $p = 2 \sin^2 \theta / (1 + \cos^2 \theta)$, ignoring the effects of the H_K distributions on the different angular dependences of moment and polarization. From 10 to 20 kOe applied field at 4.2 K, the magnetization fit yields $\Delta m = 0.019$, while the Mössbauer results yield (using $m = \cos \theta$) $\Delta m = 0.017$, in excellent agreement. Note that this calculation is essentially independent of the model of moment vs field, since the fit follows the experimental data well. For the temperature dependence of magnetization, an effective angle at 10 kOe is calculated from $\Delta m = 1 - \cos \theta$, where the Langevin function is assumed to hold to saturation. The results (Table II) are quite similar for the two techniques. In contrast, large particle γ -Fe₂O₃ shows neither enhanced paramagnetism nor Mössbauer moment canting.⁴

Since the high-field paramagnetic moment is not due to superparamagnetism but is caused by the canting in the smaller particles, a correct theoretical interpretation will not have two independent terms in the model moment-

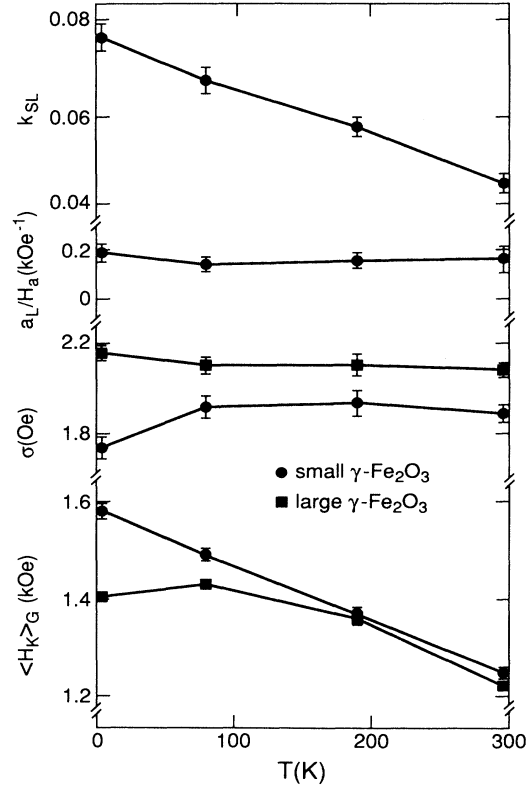


FIG. 7. Parameters from fits based on Stoner-Wohlfarth model vs temperature for small- and large-particle γ -Fe₂O₃. Lines are visual guides.

TABLE II. Effective average angle (in degrees) of spins relative to applied field direction in small γ -Fe₂O₃ in 10-kOe field as calculated by the fit to moments or Mössbauer polarization data (p).

	T (K)	
	4.2	296
Moments	16	13
p	19	13

vs-field curve. Assuming that the low-field behavior is mainly dominated by Stoner-Wohlfarth characteristics, one can extend the magnetization curves into the second quadrant to determine model coercivities (H_C). These are compared to experimental values in Table III. The model coercivities are about 30% higher than experimental, possibly indicating some incoherent rotation. However, they are in substantially better agreement than the previous calculations,¹⁹ due to the broader distributions found through the use of higher applied fields, and are far lower than theoretical predictions.²⁰ The much more rapid increase of H_C with decreasing T found in the small γ -Fe₂O₃ arises from the more rapid increase in $\langle H_K \rangle_G$. Room-temperature H_C for the treated sample was about 4% higher than for the untreated material.

Since the magnetization data show broad anisotropy field distributions, one must consider the possibility that the small polarization seen at high fields is due to the high- H_K tail in the distributions. Thus, calculations of the expected polarization have been performed for randomly oriented Stoner-Wohlfarth model particles exhibiting anisotropy field distributions. These begin with the geometrically-averaged line areas $A_j(H_a/H_K)$ for a single anisotropy field:¹⁰

$$a_j(H_a) = \frac{\sum_{H_K} P(H_K) A_j(H_a/H_K)}{\sum_{H_K} P(H_K)},$$

where a_j is the area of the j th line ($j = 1$ to 6) with given probability distribution. The composite model polarization is then found as

$$p_m = 1.5 \frac{a_2}{a_1} = 0.5 \frac{a_2}{a_3}.$$

Calculations of p_m were performed with anisotropy field distributions determined by the magnetization data, ignoring the high-field susceptibility terms. Due to the quadratic dependence of p on θ for low values of θ , the

TABLE III. Model determination of H_C compared to experimental values (units of Oe).

Sample	T (K)	Model	Experiment
Large γ -Fe ₂ O ₃	4.2	441	334
	296	390	288
Small γ -Fe ₂ O ₃	4.2	549	440
	296	416	306

polarization converges more slowly to its final value than does the magnetization as terms are added to the high- H_K tail in $P(H_K)$. Thus for the distribution spacing $\Delta H_K = 0.01 \langle H_K \rangle_G$, a few thousand terms were included. The result for small γ -Fe₂O₃ at 10-kOe applied field and 296 K is $p_m = 0.0052$, one order of magnitude below the experimental value. At 4.2 K and 10 kOe, $p_m = 0.0066$, or about 6% of the observed value. At 60 kOe, $p_m = 0.00017$, or 300 times less than the experimental value. Thus, the observed polarization is not due to the high- H_K tail in the Stoner-Wohlfarth anisotropy field distributions obtained from relatively low-field magnetization data.

The cause of the slow approach to alignment of the γ -Fe₂O₃ spins is still uncertain. One possibility is magnetocrystalline anisotropy. Analyses of high-field Mössbauer polarization data for Co-doped²¹ and Co-adsorbed²² γ -Fe₂O₃ yield H_K values reasonably consistent with the large magnetocrystalline anisotropy energies determined from low-field magnetization measurements. However, if one applies the same type of analysis to γ -Fe₂O₃, the deduced anisotropy fields are far greater than can be found for S-state Fe³⁺ ions. For example, the polarization obtained in the present work at 60 kOe and 4.2 K yields¹⁰ an equivalent uniaxial anisotropy field of 36 kOe. Smaller γ -Fe₂O₃ particles (possibly containing some Fe²⁺) with diameters less than 30 Å have been obtained by slow oxidation of iron-metal particles²³ and films.²⁴ At low temperatures, the Mössbauer spectra show essentially no deviation from random orientation in fields of 25 and 45 kOe, respectively. The corresponding anisotropy fields are in the range of hundreds of kOe.

The more likely source for the canting lies in the much larger exchange fields. The A - B , B - B , and A - A interactions are all competing antiferromagnetic. The weakening of the dominant A - B interaction by Fe vacancies on the A site, for example would lead to a local B -site spin canting. Canting occurs readily in ferrites with partial diamagnetic substitutions, and the surface of the γ -Fe₂O₃ particles was seen² as analogous. However, the current Mössbauer data show that there is no preferential surface canting.

CONCLUSION

Although there exists moment canting in the Mössbauer spectra of small γ -Fe₂O₃ particles in large applied magnetic fields, no difference is seen in the canting as a function of field and temperature between the original particles and those with 2 or 10% metal ⁵⁷Fe on the surface. The canting is therefore due to a finite-size effect, and is apparently uniform throughout the volume of the particles. Moment-vs-field data for the untreated sample and a large particle γ -Fe₂O₃ were fit with anisotropy field distributions within the Stoner-Wohlfarth model. The large γ -Fe₂O₃ particles show little additive paramagnetic susceptibility. The small γ -Fe₂O₃ exhibits a large, temperature-dependent susceptibility, which increases with decreasing temperature. Employing the formalism of a Langevin function, one finds a lack of temperature dependence in the argument, so that the suscep-

tibility does not arise from superparamagnetism. The temperature and field dependence of the high-field Mössbauer canting and the magnetic susceptibility can be described fairly well by common canting angles. There is substantial tailing in the Mössbauer hyperfine field distribution for both untreated and treated small γ -Fe₂O₃ particles, increasing with increasing temperature. Thus, part of the reduction in these hyperfine fields arises from weakened exchange interactions, presumably due to lower-coordinated near-surface atoms, as can be seen in

the enhanced tailing for the treated sample. The remainder of the reduction in hyperfine fields is also a finite-size effect. There is no evident superparamagnetic phase in the Mössbauer spectra in zero field, or from the tailing fractions, in field.

ACKNOWLEDGMENTS

This work was supported by NSF-DMR-87-07421 and IBM.

-
- ¹K. Haneda, *Can. J. Phys.* **65**, 1233 (1987).
²J. M. D. Coey, *Phys. Rev. Lett.* **27**, 1140 (1971).
³A. H. Morrish, K. Haneda, and P. J. Schurer, *J. Phys. (Paris) Colloq.* **37**, C6-301 (1976).
⁴A. H. Morrish and K. Haneda, *J. Magn. Magn. Mater.* **35**, 105 (1983).
⁵A. Ochi, K. Watanabe, M. Kiyama, T. Shinjo, Y. Bando, and T. Takada, *J. Phys. Soc. Jpn.* **50**, 2777 (1981).
⁶T. Okada, H. Sekizawa, F. Ambe, S. Ambe, and T. Yamadaya, *J. Magn. Magn. Mater.* **31-34**, 903 (1983).
⁷A. H. Morrish and K. Haneda, *J. Appl. Phys.* **52**, 2496 (1981).
⁸K. Haneda and A. H. Morrish, *J. Appl. Phys.* **63**, 4258 (1988).
⁹F. T. Parker and A. E. Berkowitz, *Phys. Rev. B* **44**, 7437 (1991).
¹⁰F. T. Parker and A. E. Berkowitz, *IEEE Trans. Magn.* **MAG-25**, 3647 (1989).
¹¹G. Le Caer and J. M. Dubois, *J. Phys. E* **12**, 1083 (1979).
¹²R. J. Pollard, *J. Phys. Condens. Matter* **2**, 983 (1990).
¹³T. C. Huang, M. F. Toney, S. Brennan, and Z. Rek, *Thin Solid Films* **154**, 439 (1987).
¹⁴C. Ortiz, G. Lim, M. M. Chen, and G. Castillo, *J. Mater. Res.* **3**, 344 (1988).
¹⁵W. Feitknecht and K. J. Gallagher, *Nature (London)* **228**, 548 (1970).
¹⁶T. Shinjo, M. Kiyama, N. Sugita, K. Watanabe, and T. Takada, *J. Magn. Magn. Mater.* **35**, 133 (1983).
¹⁷M. Kaneko, *IEEE Trans. Magn.* **MAG-16**, 1319 (1980).
¹⁸E. C. Stoner and E. P. Wohlfarth, *Philos. Trans. R. Soc. London, Ser. A* **240**, 599 (1948).
¹⁹F. T. Parker and A. E. Berkowitz, *J. Appl. Phys.* **67**, 5158 (1990).
²⁰Y. D. Yan and E. Della Torre, *J. Appl. Phys.* **66**, 320 (1989).
²¹P. E. Clark and A. H. Morrish, in *Magnetism and Magnetic Materials—1973 (Boston)*, Proceedings of the 19th Annual Conference on Magnetism and Magnetic Materials, edited by C. D. Graham and J. J. Rhyne, AIP Conf. Proc. No. 18 (AIP, New York, 1974), p. 1412.
²²Q. A. Pankhurst and R. J. Pollard, *Phys. Rev. Lett.* **67**, 248 (1991).
²³K. Haneda and A. H. Morrish, *Surf. Sci.* **77**, 584 (1978).
²⁴T. Shinjo, T. Iwasaki, T. Shigematsu, and T. Takada, *Jpn. J. Appl. Phys.* **23**, 283 (1984).